Importance of Ground Strain in Predicting Blast Induced Strain and Stress in Pipelines

C.H. Dowding
Northwestern University, Evanston, Illinois USA

U.G. Akkaya
Istanbul University, Istanbul, Turkey

ABSTRACT: This paper compares measured ground motions and strains in welded, steel pipelines, which were induced by blasting at unusually small-scaled distances. All three studies involved field measurement of the blast response of large (20 to 36 in. or 500 to 900 mm) diameter, pipelines trenched into or placed immediately above rock. Motions were induced by detonations of 5 to 15 lbs (2 to 7 kg) per delay trenching shots and 800 to 900 lbs (360 to 400 kg) per delay surface mining shots. Some of the blasts were detonated as close as 4 ft (1.3 m) from the pipeline. All of these field-scale blasts were detonated at scaled distances less than 30 ft/ ($lb^{1/2}$) or 13.5 m/($kg^{1/2}$). More than 30 of the blasts produced peak strains greater than 10 micro mm/mm, and peak particle velocities greater than 1 ips (25 mm/s); some of which were higher than 10 ips (250 mm/s). These measurements demonstrate the importance of absolute distances between pipe and blast, depths of blast hole, proper measurement of propagation and particle velocity, measurement of both hoop and longitudinal strains, equality of ground and pipe strains, and conservativeness of typical regulatory particle velocity control limits.

INTRODUCTION

This paper compares in a consistent fashion three studies involving intensive measurement of strains in welded steel pipelines at induced by blasting at unusually small-scaled distances. As such it is one of the largest suites of such responses in the world. All three studies involved field measurement of the blast response of large (20 to 36 in. or 500 to 900 mm) diameter, welded steel pipelines trenched into or placed immediately above rock. All of the blasts involved field-scale charges per delay. Charges per delay included 5 to 15 lbs (2 to 7 kg) per delay trenching shots and 800 to 900 lbs (360 to 400 kg) per delay surface mining shots. Some of the shots were detonated as close as 4 ft (1.3 m) from the pipeline. All totaled, compared are some 50 measurements of strains produced by field scale blasts at scaled distances less than 30 ft/$lb^{0.5}$ (13.5 m/$kg^{0.5}$). More than 30 of the blasts produced peak particle velocities greater than 1 ips (25 mm/s); some of which were higher than 10 ips (250 mm/s). Some 40 of the blasts produced strains greater than 10 micro mm/mm.

This comparison had not been conducted previously for a number of reasons. The Southwest Research Institute (SwRI) trenching study (Esparza et al, 1991) was not integrated into the 1981 SwRI base line work involving model tests in soil. The US Bureau of Mines (USBM) study (Siskind et al, 1994) was conducted after both the SwRI studies and thus could not have been included. The VME study (Sharifinassab & Clark, 1984) was never fully published and was exhumed from unpublished project files.

In addition to comparing peak strains in both the longitudinal and circumferential directions, time histories of these orthogonal responses were compared for a half dozen of the largest blasts and/or largest strain responses for which such information remained.

Comparisons are multiple

1. Peak Particle Velocity (PPV) attenuation relationships are compared to each other via comparison with the Oriard's (2002) expected attenuations relations.
2. Strain and PPV attenuation relationships are compared on the same scaled distance graphs for all three studies to illustrate the effects of geology and shot type on the attenuation of each with respect to scaled distances.
3. Measured strains are compared to those predicted by pipe compliant ground strains (Nyman, Dowding, Oriard -2008 -NDO)
4. Maximum stresses, calculated by three different approaches are compared for each study. They are calculated via two methods involving scaled distance: 1) SwRI scaled distance formula and 2) the NDO compliant ground strain approach, and compared to those calculated from measured hoop and longitudinal strains employing the biaxial strain formula.

1. OVERVIEW OF THREE STUDIES

Blast Hole, Trench, Shot Design, and Instrumentation

Details of the three studies are compared in Table 1 and the shot geometries are compared in Figure 1. As can be seen in Figure 1, the blasting geometry of the USBM surface mining study differs radically from that of the trenching geometry of the SwRI and VME studies. The 800 to 900 lb per delay detonations associated with mining result in large stand-off distances from the pipeline. Even though the scaled distances are similar for the three studies, the stand-off distances for the mining shots are large in an absolute and wave length scale. The resulting strain time histories from these mining shots for unusually small-scale distances differ from those of the trenching studies.

Geology is rock dominated. Ground motions travel mainly through rock for all three studies as all three trenches are shallow relative to the depth of blast holes in rock. The two trenching studies involve blast hole depths that are 2 to 3 times deeper than the pipeline trenches. The mining study blast holes are some 12 times deeper than the trenches. In addition the depth of soil overburden is small compared to the trench depth, which further constrains the ground distortion to that of the rock. Only in the mining study was the overlying soil thicker than the trench, and then it was only 1 to 2 feet (0.3-0.7 m) thicker. This thin soil cover most likely moves along with the rock, as no reasonable wave length disturbance can travel only through the thin soil overburden.

Rock type varied considerably. The USBM mining study involved shots in shale. While the SwRI trenching study did not identify the rock type photographs indicate that it was unlikely to be sedimentary. It was most likely igneous. The VME study also did not identify the rock type, and unfortunately there were no photographs to allow visual identification. However, this study was conducted for a Seattle municipality, so the rock type is likely to be either igneous or metamorphic.

In all three of the studies the pipes were constructed of welded steel with a Young's modulus of 29×10^6 psi (210 GPa). Wall thicknesses varied between 0.26 inches (6.3 mm) (USBM) to 0.31 inches (7.6 mm) (VME) to 0.47 inches (11.5 mm) (SwRI). Yield strengths varied between 42 and 56 kips per square inch (300 to 400 MPa).

Table 1. Shot, trench, and pipe geometry (1 ft = 0.305 m, 1 in. = 25.4 mm, 1 lb = 0.454 kg, 1 ksi = 6.895 kPa)

	Number holes	Depth holes	Diameter holes	Burden/ spacing	W total	Typical number delays	Delay interval	Explosive type	W per delay min.	W per delay max.	Rock type	Depth of trench	Soil thickness	Pipe Diameter	Pipe Wall Thickness	σ_{yield}
	Average	ft	inch	ft	lb		ms		lbs	lbs		ft	ft	inch	inch	ksi
Esparza	15	16	3	6/6	~225	15	25	60% extra gelatin	15	20	Igneous	~5	<5	30	0.47	?
USBM	50	40-65	10-12	15/15	~100	20	126-row 25-hole	ANFO?	668	964	Shale	~5	7	20	0.26	56
VME	6	10	?	varies	15-50	2		?	5	19.5	?	~5	2	34	0.31	42

Shot designs varied considerably. As shown in Figure 1, hole depths for the mining study were some 66 feet (20 m) deep while those for the trenching studies were only some 6 feet (1.8 m) deep. None of the shots involved any decking. In other words each blast hole was detonated all at once. Only the VME study involved more than one hole detonated at the same delay. Although the use of ¾ to 1 second delay intervals in the VME study resulted in non-simultaneous detonation in several instances. The other studies employed standard 25 millisecond delay intervals between single blast hole detonations.

Instrumentation was relatively similar. Strains were measured with wire strain gages in all of the studies. Both weldable and epoxy mounted gauges were employed in the USBM study. Although not described explicitly, it appears that the strain gages were epoxy mounted for the SwRI study. The VME study employed weldable gages. All three studies employed standard blast vibration seismographs. Unless modified, standard seismographs may not return sufficiently accurate readings in particle velocity environments above 5 ips. This observation will be discussed in greater detail in later sections.

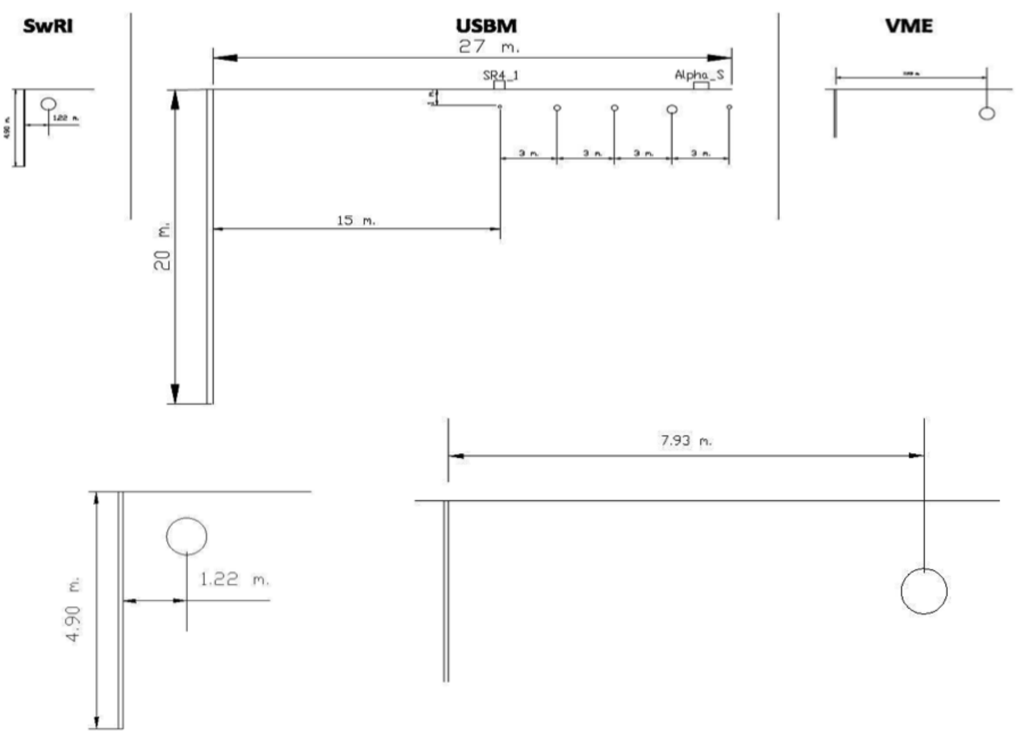

Figure 1. Top: Cross-sections of blasts for the three studies at same scale. Bottom: Closest SwRI and VME blasts enlarged. The SwRI geometry is for shots 19-21, which were within the crater zone.

2. COMPARISON OF PEAK RESPONSES

2.1 *Peak Particle Velocity*

Attenuation relations for the three studies are compared in Figure 2 with that expected (Oriard, 2002). The lower and upper bounds are represented by the two solid lines denoted by the equations y = 24 and 242 times scaled distance (SD) to the -1.6 power. Peak particle velocity (PPV) is the y-axis and scaled distance is the x-axis. Scaled distance is the stand-off distance to the nearest blast hole, R, divided by the square root of the maximum charge per delay, W. These graphs are plotted on a log-log grid, which returns a straight line for a power relationship shown by the Oriard bounds.

The studies are arranged by SwRI on the left, USBM in the center, and VME on the right. This order will be maintained throughout the discussion. As described earlier, the USBM blasts were those from surface coal mining and involved charges per delay of some 850 lbs (400 kg) per delay, while the SwRI and VME studies reflected trench type construction with some 5 to 15 lbs (2 to 7 kg) per delay.

Scaled distances can be confusing and possibly misleading when comparing radically different shot types. While the scaled distances will be roughly the same for the trench and surface mining shots in these comparisons, the absolute distances will differ significantly. For instance at a scaled distance of 10 ft/lb$^{0.5}$ (4.5 m/kg$^{0.5}$), the absolute distance for a trench shot would be 30 feet (9 m) for a shot with a charge per delay of 10 lbs (4.1 kg). At the same-scaled distance the stand-off distance for a surface mining shot would be 300 feet (91 m) for a charge per delay of 850 lbs (390 kg). These differences in scale are best understood by comparing the cross sections of the shot geometries in the three studies shown earlier in Figure 1.

Rates of attenuation and amplitudes of PPV are a function of geology, shot geometry and initiation sequence. While the PPV from SwRI and USBM decays at the expected rate, the amplitudes differ. This difference results from the large differences in the excavation geometry and blasting for the two cases. The PPV in the VME study decays more rapidly and has a higher amplitude at the same scaled distance than the other two studies. This difference may be a function of the delay type. Time history records show that there are full seconds between detonations in the VME study. This long delay indicates that the blasts may have involved tunnel delays rather than the more standard millsecond delays. None of the three studies involved the newer and much more accurate electronic delays.

In both the SwRI and USBM studies PPV's at scaled distances below 5 ft/lb$^{0.5}$ (2.2 m/kg$^{0.5}$) fall below the attenuation slope projected from larger scaled distances. There may several reasons for these low PPV's. The velocity transducers in the SwRI study may not have been able to respond above 4 to 5 ips (100-125 mm/s). Many velocity "geophones" "pin-out" at PPV around 4 ips. Explanation of the fall off for the USBM shots at small scaled distances may be a result of digitizing rates that may not have been fast enough to catch the time history. PPVs for shots 9 and 10 in the VME study are also low. Both of the velocity transducer issues pertaining to the SwRI and USBM study apply to the VME study. The effect of shot design will be discussed later in the section dealing with time histories.

2.2 Maximum Strains

Despite the fall off of the measured PPV's at small-scaled distances, Figure 3 shows that the strains in all three studies continue to increase according to a power function. Equations of these functions are shown on the plots. The y-axis on these graphs represents both PPV and maximum strain and requires an explanation. The whole numbers have different decimal values. The PPV whole numbers are in inches per second. The strains are micro-strains or 10^{-6} times the whole number. Thus shot 19 in the SwRI study produced a PPV of 5 ips (125 mm/s) and a strain of some 180 micro-strain.

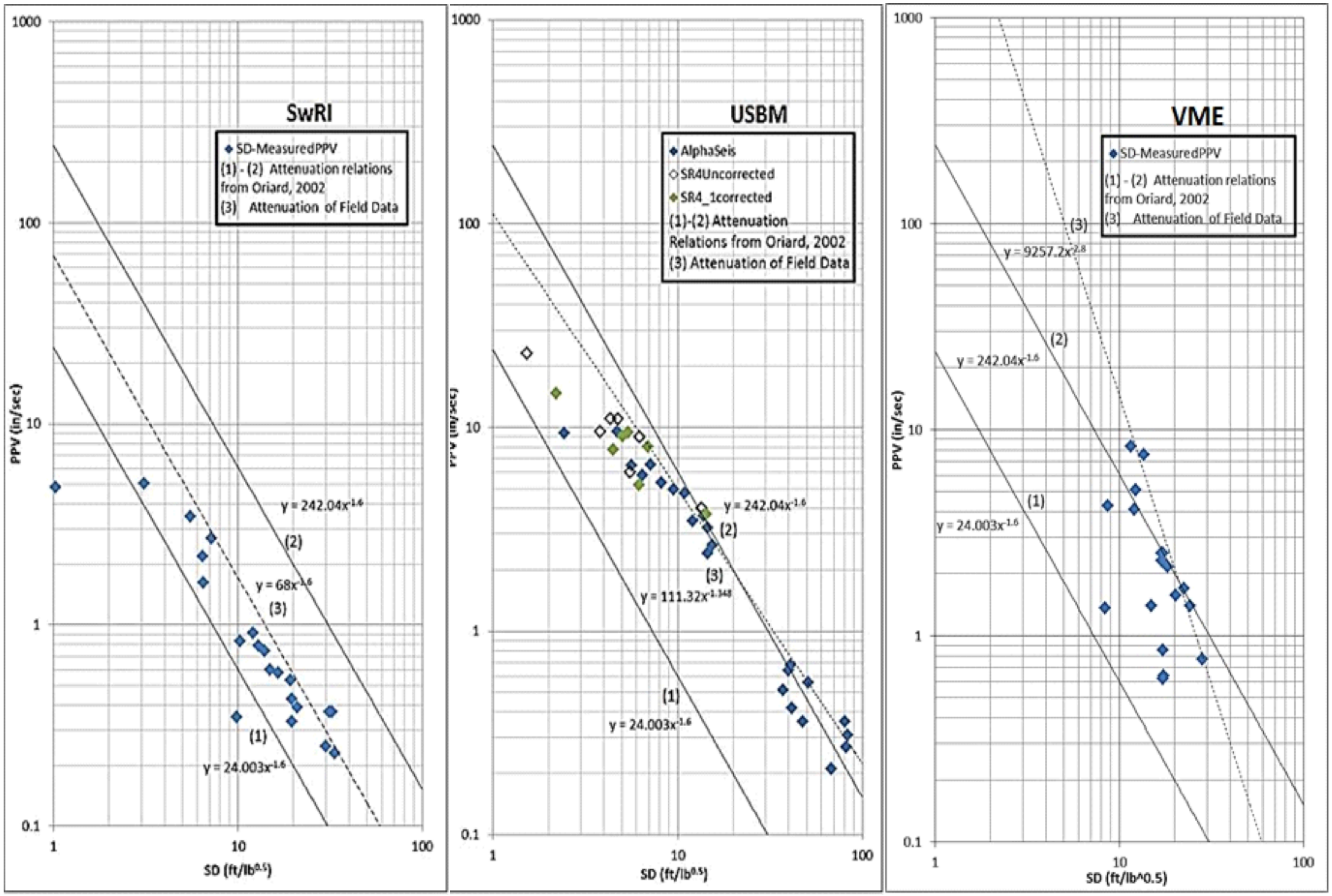

Figure 2.

Comparison of the attenuation of peak particle velocity (PPV) with scaled distance for the three studies. The differences compared to the Oriard bounds of expectation demonstrate the effects of shot type, geometry, and geology. (1 in/sec = 25.4 mm/s; 1 ft/lb$^{0.5}$ = 0.45 m/kg$^{0.5}$)

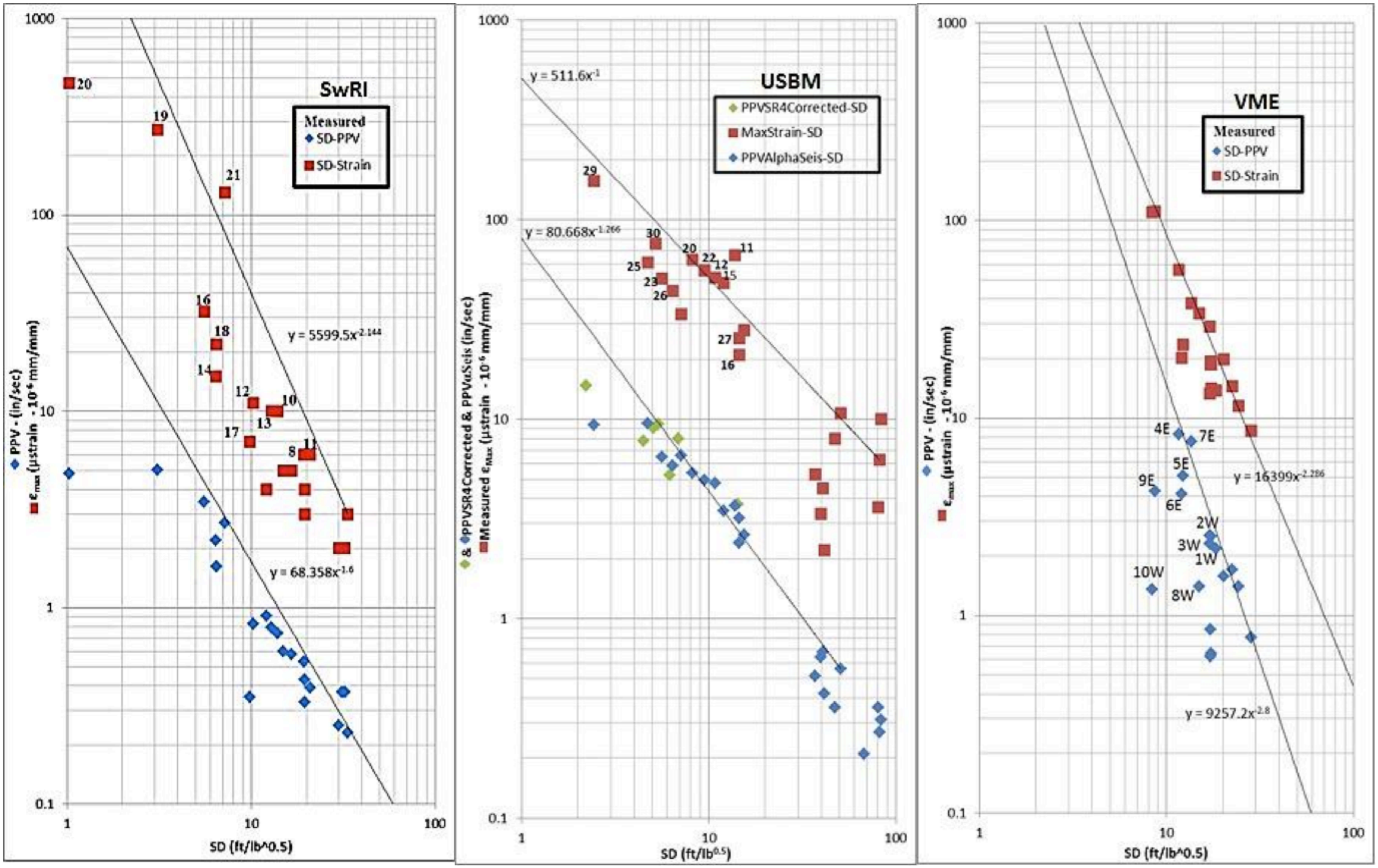

Figure 3. Comparison of the attenuation of maximum strain (hoop or longitudinal) and peak particle velocity with scaled distance for the three studies. While the integer values can

be plotted on the same y-axis scale, their dimensions and powers differ. PPV is in in/sec x 10^0 and strain is in mm/mm x 10^{-6} (micro-strain). (1 in/sec = 25.4 mm/s; 1 ft/lb$^{0.5}$ = 0.45 m/kg$^{0.5}$)

For the most part maximum strains at small scaled distances continue to follow the power law determined from scaled distances greater than 10 ft/lb$^{0.5}$ (4.5 m/kg$^{0.5}$). There are only two shots (both in the SwRI study) that do not follow that observation in this suite of data. The two exceptions are shots 19 and 2. These two shots and shot 20 were detonated within 4 ft (1.25 m) of the pipeline and one quarter of the 16 ft deep blast holes. As will be discussed later, this geometry places the pipeline in the crater zone, and thus requires special, prudent design as described by Oriard (2002). Maximum strains at small-scaled distances continue to follow the power law attenuation relationship in both the USBM and VME studies. Although not shown on these graphs the same would be true for hoop strains for the SwRI study.

2.3 Maximum Stresses

Blast induced stresses calculated through three different methods are compared for the three studies in Figure 4; left to right; SwRI, USBM, VME. Since only deformation or strain can be measured, stresses must be calculated no matter the approach. Stresses cannot be directly measured. Some approaches to calculating stress are more direct and more closely related to the strain, which is measured. The calculation most closely related to the measured strain is that calculated by the biaxial stress-strain relationship, which is represented by the black filled circles in Figure 4. The equation shown in the key demonstrates the use of the hoop and longitudinal strains (ϵ_{hoop}, ϵ_L) in combination with the modulus of elasticity, E, and Poisson's ratio, ν. In this study the maximum strains, no matter the time of occurrence during passage of the blast wave or its sign value (positive or negative) are added to calculate the stress. As will be shown later in the section on time histories, use of non-time correlated strain peaks without regard to sign is conservative.

The other two methods of calculating maximum stress are both based upon some type of scaled distance relationship. The Southwest Research Institute (SwRI) method, the current industry standard in the United States, is represented by the open circles in Figure 4. Stresses calculated through the compliant ground strain approach are represented by the filled squares. This method is explained in detail in Nyman, et al, (2008) and will be abbreviated as NDO.

The SWI approach employs the explosive weight per delay, W, the stand-off distance, R, the steel modulus of elasticity, E, the pipe radius, h and a weight factor to account for different types of explosives, n (=1 in this study). It does not account for differences in geology (e.g. rock vs. soil) or shot relief (trenching vs. surface mining). Thus the open circles are all in the same straight line in the three studies. This straight line is shifted upward or downward slightly to account for differences in E and h.

The NDO method employs PPV from the scaled distance relationships in Figure 2 to estimate strains from the relations shown in the bracketed section of the key. The PPV-strain relationship is based upon the assumption that the steel pipe is more flexible than the surrounding ground as discussed in Nyman et al (2008). The strains are a function of the incident angle, Θ, and the propagation velocity of the compressive and shear waves in the surrounding medium, C_c & C_s. Since the NDO approach in this study is also based upon the scaled distance by virtue of the extrapolation of PPV from scaled distances greater than 10, the squares tend to follow a linear trend with differences due only to incident angle

PPV's and C_c & C_s for the NDO calculations were estimated from the measured data. As discussed above, the PPV's at scaled distances less than 5 ft/lb$^{0.5}$ were estimated from values measured at larger scaled distances. PPV measurements at scaled distances where PPV should have been greater than 5 ips for the SwRI and VME studies are suspect because of transducer problems as described above. The USBM study addressed these issues and employed systems to more reliably measure PPV's up to 10 ips.

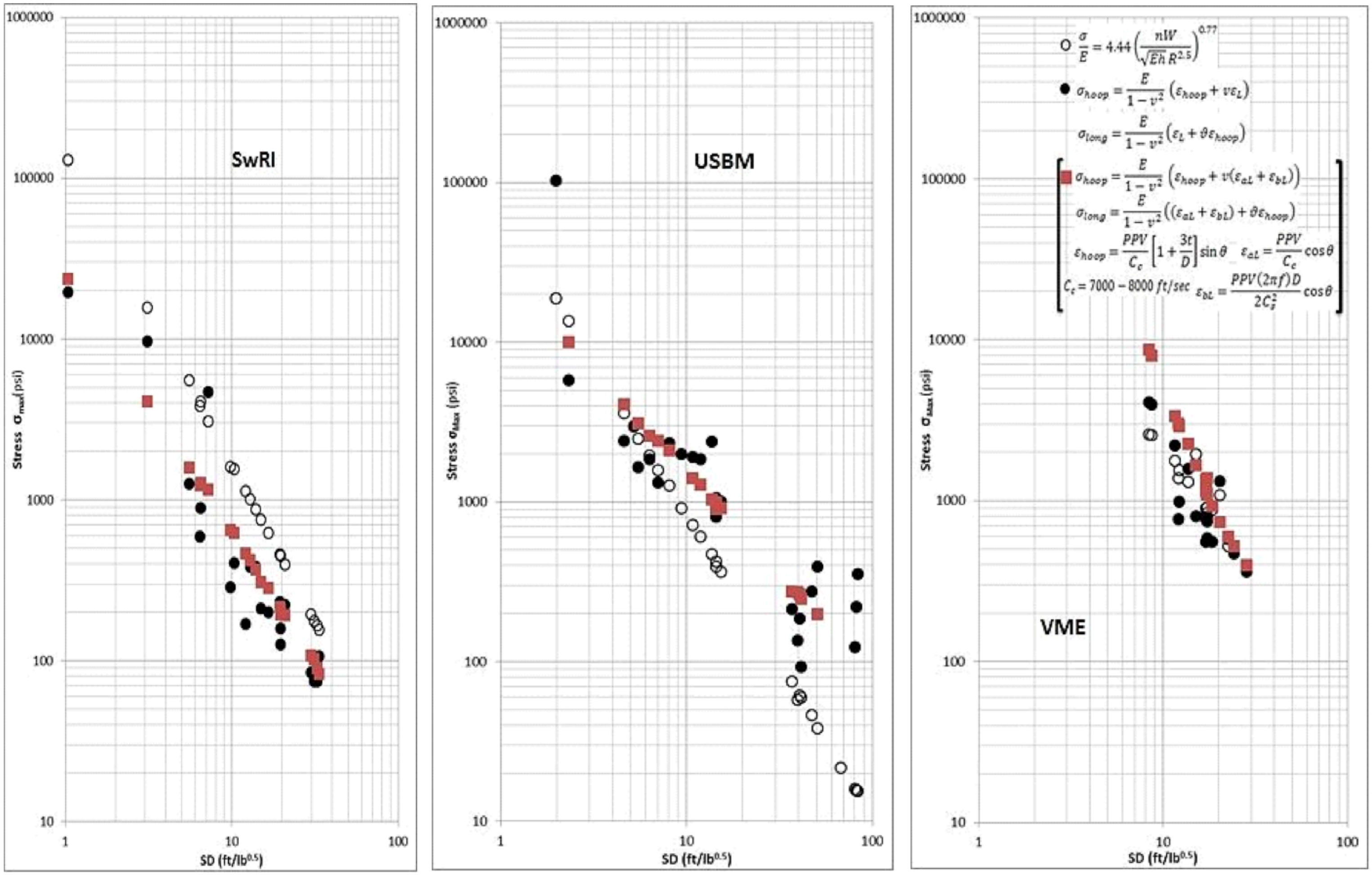

Figure 4. Comparison of the attenuation of calculated stress with scaled distance for the three studies. The SwRI-scaled distance method is shown by the open circles and the compliant ground strain method is shown by the filled squares. Both of these calculations were made in a predictive mode without reference to measured data. Since stresses cannot be measured directly, these two predictive methods are compared stresses calculated from measured stains with the biaxial stress-stain assumptions. (1 in/sec = 25.4 mm/s; 1 ft/lb$^{0.5}$ = 0.45 m/kg$^{0.5}$)

None of the three studies measured propagation velocity C_c & C_s. Compressive wave propagation velocity, C_c, was estimated by dividing the measured PPV by the measured strain at scaled distances of greater than 10. Shear wave propagation velocity, C_s, was assumed to be ½ that of the compressive wave. Resulting values of C_c ranged from 7000 to 8000 ft/sec. This approach is based upon a plane wave assumption as described in Dowding (1996). The plane wave assumption requires that the distance between detonation and receiver is sufficiently large so that the wave engulfs the receiver with a wave front of limited curvature.

Figure 5 compares graphs of the three calculations of stress but NDO without consideration of the angle of incidence. A comparison of Figures 4 and 5 shows there to be less change in the results than might be anticipated.

Comparison of the stresses calculated for the three cases shows the SWI approach to be less able to account for changes in blasting details. The open circles are have much smaller variation across the three studies than do the closed circles that represent stresses calculated directly from strains measured on the pipes. The NDO approach follows the variation more closely because it employs the measured PPV's and thus involves consideration of the medium through which the blast wave travels as well as the shot type. Both approaches can be employed as long as their limitations and those of the instruments are understood.

3. TIME HISTORIES OF PARTICLE VELOCITY AND STRAIN

Much information is contained in time histories of ground motion and strains given the multi-delay nature of blast induced transient excitation. To illustrate this information time histories of particle velocity and strain for several of the USBM shots are compared in Figure 6. Strain time histories are shown on the top and particle (ground) velocity time histories are shown on the bottom. Time scales are the same for both. All time histories last for one second. Time-correlated strain responses to ground motions for shots 25 and 27 can be observed because the time scales and zeros are the same for the upper and lower graphs. Two components of strain are measured, longitudinal – L- (parallel to the pipelines long axis) and circumferential or hoop –H- (perpendicular to the pipelines long axis). These two components are aligned along the principal directions of distortion. Three dimensional ground motion is measured in three components, L,V& T. The frame of reference for ground motion is the path from the shot to the pipe and L is the radial direction and T is perpendicular to L. For most geometries, T is assumed to be nearly aligned in a direction parallel to the long axis of the pipeline.

As can be seen in Figure 2 and 6, shot 25 (840 lbs per delay at 164 ft) produced greater peak particle velocity and strain than did shot 27 (670 lbs at 520 ft). Individual pulses from the individual delays for shot 25 are evident in the vertical component of the particle velocity wave train. They are approximately 25 milliseconds apart, which confirms the 25 millisecond delay shot design. The higher frequency pulses, which dominate the particle velocity for shot 25 have attenuated in shot 27.

Strain seems to follow the lower frequency L velocity component as can be seen by peaks in both time histories at roughly 0.3, 0.5 and 0.7 ms. Both strain time histories for shots 25 and 27 are pulse dominated. There was only one other shot – 29- at a significantly smaller stand-off distance, 50 ft (15 m). This small distance is within the crater zone, but unfortunately there is no time history reported for that shot.

It is instructive to investigate the timing of the Land H strain peaks. As described above, stresses are normally and were calculated in this study as though the maximum strains in the L and H directions occur at the same instant of time and have the same sign. Strain peaks at 0.3, 0.5 and 0.7 seconds have the opposite sign. L's are positive and H's are negative. If this difference in sign were taken into account the calculated stresses would be considerably lower. This opposite sign is seen to be the same for all three of the strain time histories for the USBM study.

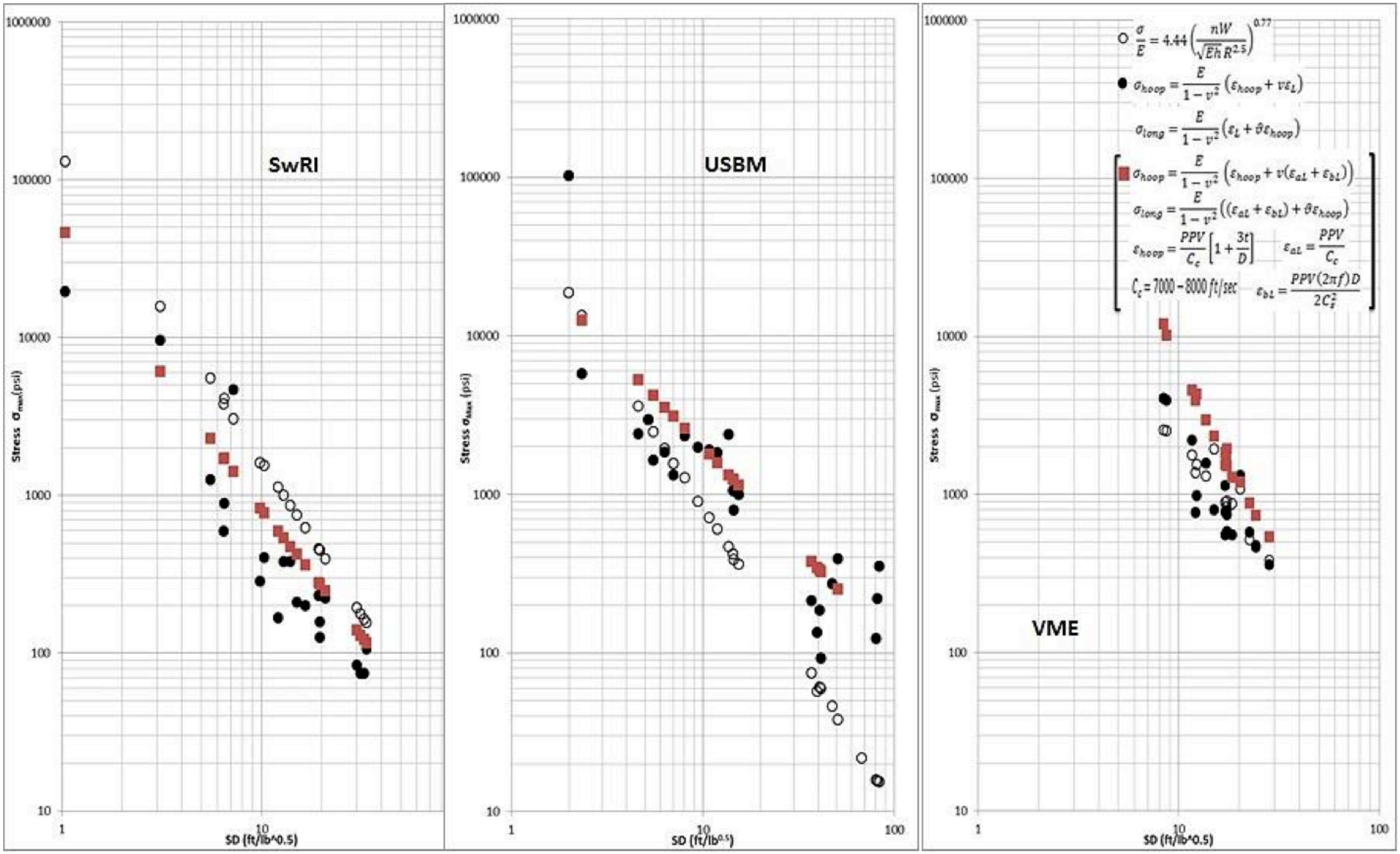

Figure 5. Comparison of the attenuation of calculated stress with scaled distance for the three studies without the consideration of the incident angle for the compliant strain approach. Elimination of the incident angle increases the calculated stresses via the compliant strain calculation. (1 in/sec = 25.4 mm/s; 1 ft/lb$^{0.5}$ = 0.45 m/kg$^{0.5}$)

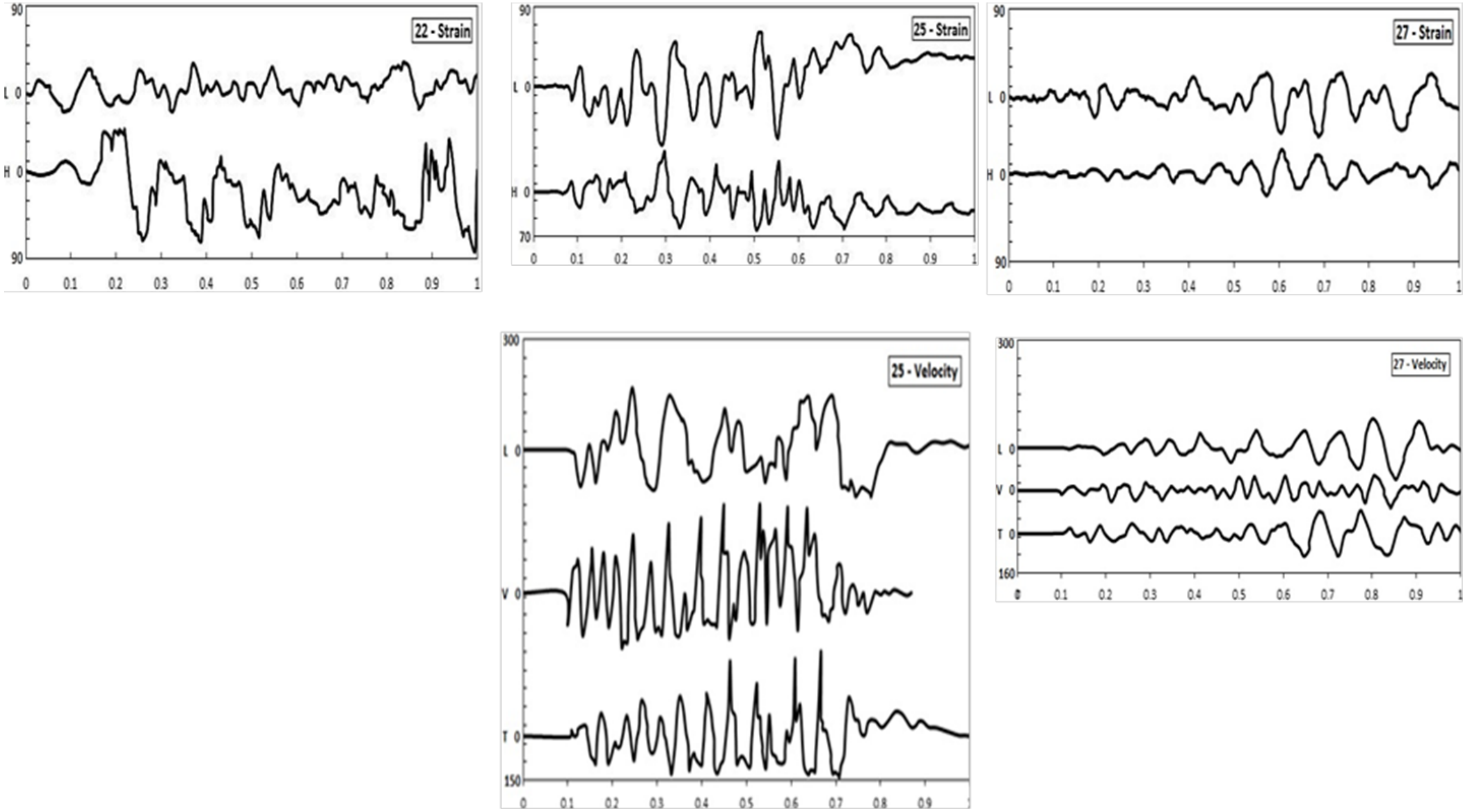

22 - Strain
25 - Strain
27 - Strain
25 - Velocity
27 - Velocity
L 0
H 0
V 0
T 0
90
70
300
150
160
0 0.1 0.2 0.3 0.4 0.5 0.6 0.7 0.8 0.9 1

Figure 6. Comparison of large strain and particle velocity time histories from the USBM study at the same scale; top, strain; bottom, particle velocity on ground surface. Strains time histories follow the velocity time history pattern induced by the delay initiation sequence for shots further distant than 1 blast hole depth. (y-axis strain scale, 20 µmm/mm per tick mark; y-axis velocity scale, 50 mm/s (2 ips) per tick mark; x-axis time scale, 0.1 seconds per tick mark)

Figure 7 compares strain time histories for shots 14 and 20 in the SwRI study. There were no particle velocity time histories at the 30 in (760 mm) diameter pipeline in the SwRI report. As with the USBM study the strain and time scales are the same. The strain time history of shot 14 shows the pulsing pattern seen with the USBM study. The time history for shot 20, with a stand-off distance of only 4 feet (1.2 m) is dramatically different. There is only one pulse. This pulse is probably from the blast hole closest to the stain gage. Its large amplitude may have swamped the response produced by other, more distant blast holes. The H and L components still do not coincide in time.

This single pulse time history is the same as those measured by SwRI in their small-scale soil model tests. As discussed before, this hole geometry shown in Figure 1, is well within the crater zone. Similar time histories have been observed by SwRI (1991) in other studies at distances of 12.5 ft (3.8 m) and charges per delay of 6 to 27 lbs (2.7 to 12.3 kg) per delay Blast hole depth and relief was not given.

Strain and particle velocity time histories for shots 9 and 10 in the VME study are compared in Figure 8. These time histories were produced by shots that were detonated at a distance of 37 to 41 feet (11.2 to 12.5 m) and employed 5 to 6.5 lbs (2.3 to 3.0 kg) per hole, but with 3 holes detonated with the same long delay. The small amount of shot design information inhibits comparison between shots. However, it can be said that once again the signs of the strain peaks are opposite, and underscore the conservativeness of calculating total stress with the biaxial strain relationship discussed above.

4. CONCLUSIONS

1. Peak particle velocity (PPV) correlates with strain for PPV's less than 250 mm/s (10 ips) and/or scaled distances greater than 5 ft/lb$^{0.5}$ (2.25 m/kg$^{0.5}$).
2. At scaled distances smaller than 5 ft/lb$^{0.5}$ where the PPV-strain correlation breaks down, the absolute distances are less than the depth (length of the blast hole). Blasting at this close a distance places the pipeline in the crater zone, which is not recommended.
3. There was only one exception to the scaled distance (SD) smaller rule and that occurred where the blast was at a smaller scaled distance from the pipe but not the strain gage.
4. The geometry associated with the exception to the use of the compliant strain assumption and measured PPV's for SDs greater than 5 ft/lb$^{0.5}$ (2.25 m/kg$^{0.5}$) (or absolute distances less than the blast hole depth) requires further study. However; at these small scaled distances, the main consideration becomes the possibility of permanent displacement or cratering.
5. The compressive particle velocity employed with the NDO calculation of strain and then stress varied between 7000 and 8000 ft/sec (2,100 to 2,400 m/s). It is based upon comparison of the strain and PPV at a scaled distance of 10 to 20 ft/lb$^{0.5}$ (4.5 to 9 m/kg$^{0.5}$).
6. The propagation velocities employed in this retrospective study were not independently measured. Future research is needed to determine the best methods to measure the propagation velocity that allows strain and PPV to be related.
7. Consideration of the propagation velocity of the blast wave is a necessary component of the compliant ground strain approach. Its inclusion allows the medium to be taken into account.
8. Differences in shot type can be taken into account through use of field measurements of PPV. These field measurements are best taken at scaled distances greater than 10 with common blast vibration seismographs to assure proper measurement that can be extrapolated to smaller scaled distances.
9. The SRI scaled distance approach to calculating peak stress appears not to be always conservative in comparison to calculating stress from measured strains with the biaxial formula. This conclusion is based upon application with the USBM study.

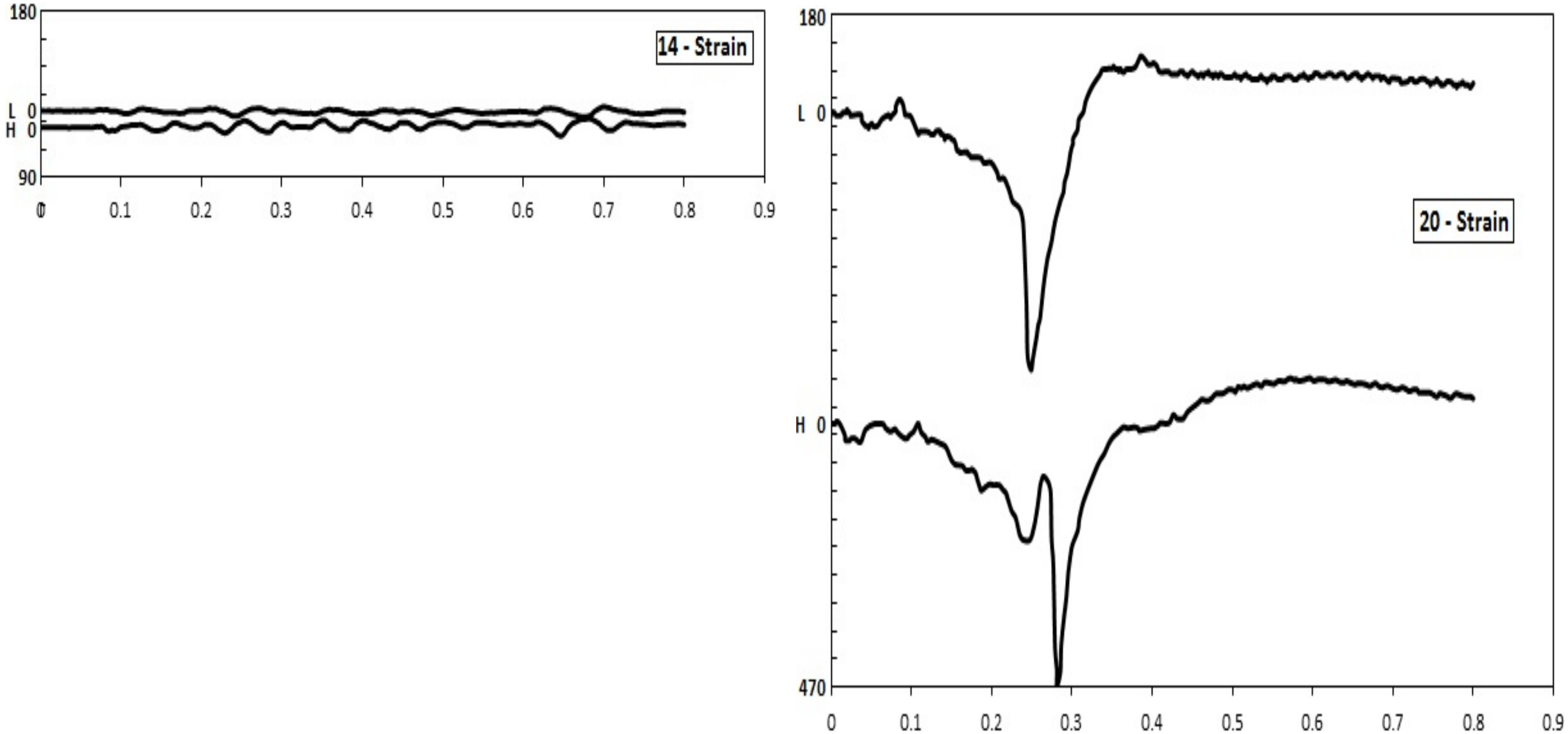

Figure 7. Comparison of strain time histories from the SwRI study for shot more distant than one blast hole depth (shot 14) with that for shot 20, which was detonated within 4 ft of the pipeline as shown in Figure 1. The response is dominated by the single pulse, which probably arises from the nearest blast hole. (y-axis strain scale, 50 µmm/mm per tick mark; x-axis time scale, 0.1 seconds per tick mark)

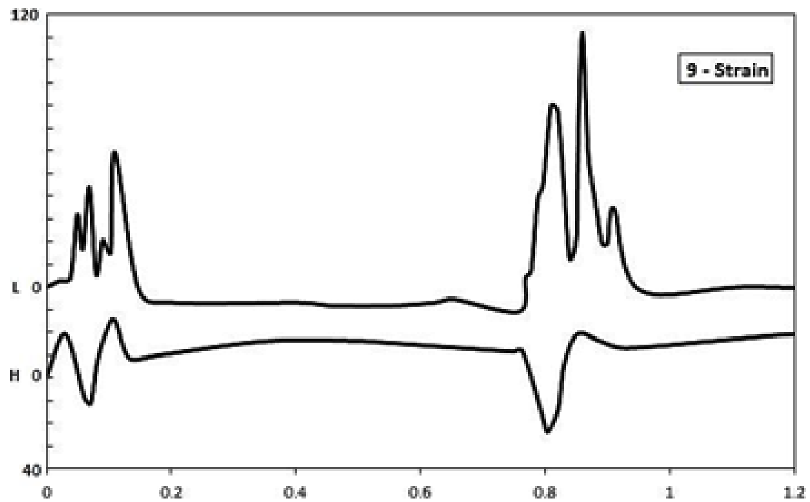
9 - Strain
120
L 0
H 0
40
0
0.2
0.4
0.6
0.8
1
1.2

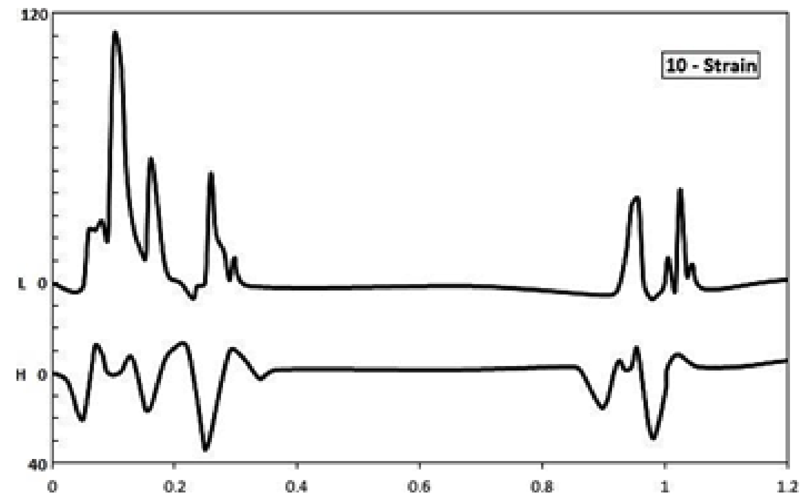
10 - Strain
120
L 0
H 0
40
0
0.2
0.4
0.6
0.8
1
1.2

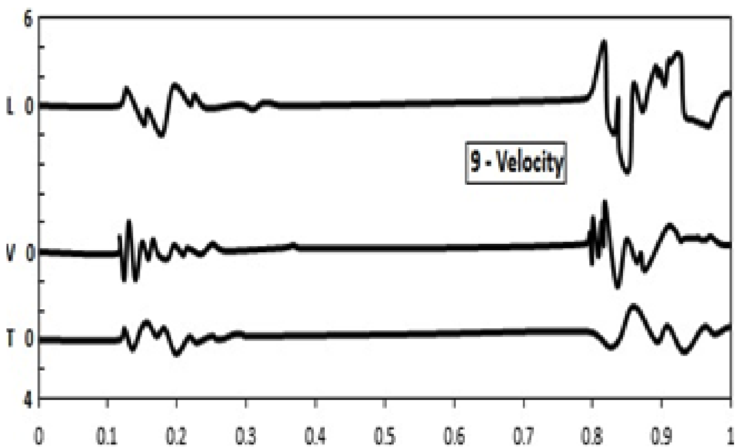
9 - Velocity
6
L 0
V 0
T 0
4
0
0.1
0.2
0.3
0.4
0.5
0.6
0.7
0.8
0.9
1

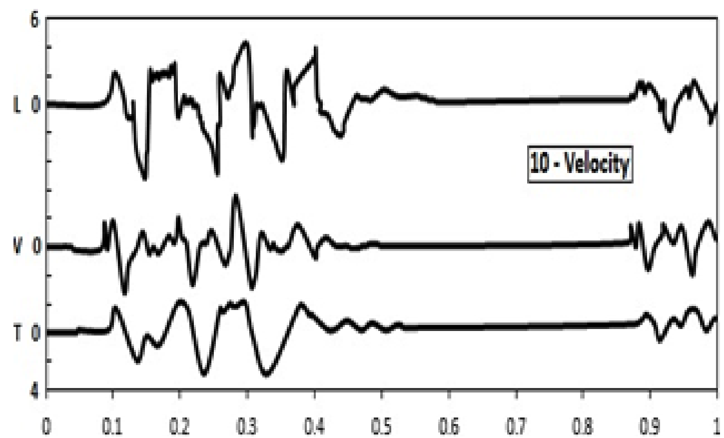
10 - Velocity
6
L 0
V 0
T 0
4
0
0.1
0.2
0.3
0.4
0.5
0.6
0.7
0.8
0.9
1

Figure 8. Comparison of large strain and particle velocity time histories from the VME study at the same scale; top, strain; bottom, particle velocity on ground surface. As with the USBM study and the distant SwRI shots, trains time histories follow the velocity time history pattern induced by the delay initiation sequence for shots more distant than 1 blast hole depth. (y-axis strain scale, 10 µmm/mm per tick mark; y-axis velocity scale, 50 mm/s (2 ips) per tick mark; x-axis time scale, 0.1 seconds per tick mark)

10. Comparison of time correlated time histories of strain shows that the longitudinal and circumferential strains often have opposite signs at their peak for pulsing time histories. Thus the assumption that they are additive (have the same sign) that is inherent in use of the biaxial strain equation is conservative. The conservativeness is large.
11. All of these studies were conducted before the use of electronic detonators. Thus there is a large probability that the designed scaled distance may not have been achieved.

5. ACKNOWLEDGEMENTS

The authors are grateful for those organizations and individuals who have provided sufficiently detailed shot and ground motion data as well as time histories that allowed this detailed comparison; E. D. Esparza of the Southwest Research Institute, D.E., Siskind of the US Bureau of Mines, and M. Sharifinassab and D. Clark of VME. While these organizations and individuals have been referenced, they are commended for their foresight in the preservation of the original data, which made this detailed comparison possible. The authors would also like to acknowledge the partial support of the Pipeline Research Council and for their continued interest in the subject of the response of pipelines to close-in blasting.

6. REFERENCES

Dowding, C.H., 1996. Construction Vibrations, Prentice Hall. Now available through ISEE and Amazon.com

Esparza, E. D, 1991. “Pipeline Response to Blasting in Rock,” Southwest Research Institute, Report for Pipeline Research Committee, American Gas Association, September 1991, 68 pp.

Nyman, D., C.H. Dowding, and L.L. Oriard, 2008. “Evaluation of Close-in Blasting Effects on Welded Steel Pipelines”, International Pipeline Conference 2008, ASME, Calgary, Canada.

Oriard, L.L., 2002. “Explosives Engineering,” Construction Vibrations and Geotechnology, International Society of Explosives Engineers, Cleveland, OH, USA.

Sharifinassab, M. and Clark, D.A., 1984. “Experimental Study of Steel Pipeline Response to Buried Explosive Detonations,” VME Nitro Consultants, Inc., Louisville, KY, USA.

Siskind, D. E., M. S. Stagg, J. E. Wiegand, and D. L. Schulz, 1994. “Surface Mine Blasting Near Pressurized Transmission Pipelines,” Report RI-9523, U. S. Department of the Interior, Bureau of Mines.